COMPUTATIONAL PROBLEMS OF ELECTRICAL ENGINEERING
Vol. 4, No. 1, 2014

INTERRELATED PROCESSES OF LOCAL ELECTRIC FIELD AMPLIFICATION IN SOLID DIELECTRICS, CONTRIBUTING TO THEIR DEGRADATION

Maksym Shcherba
"Kyiv Polytechnic Institute" National Technical University of Ukraine, Kyiv, Ukraine
m.shcherba@gmail.com

Abstract. The complex processes of local disturbance of an electric field, as well as the amplification of electrical strength and mechanical and thermal intensities in the solid dielectric, depending on the configuration of its conducting micro-inclusions are described. The analysis of the increase of maximal field strength, stressed volume, electromechanical pressures, forces, and the total current density in the cross-linked polyethylene insulator as the main factors determining the deterministic and stochastic processes of its degradation in the strong disturbed harmonic electric field is performed.

Key words: electric field amplification, dielectric, water micro-inclusion, water tree, strength, tensed volume, force, current density.

1. Introduction

The appearance of the single conducting micro-inclusions and micro-juts, groups of closely located micro-inclusions as well as initiation and development of a water tree in a solid dielectric are recognized as the main causes of local amplification of an electric field (EF) and degradation of such dielectric [2–6, 8].

There is an increased density of the induced electric charge on the tips on the surface of conducting micro-defects, that results in increase of EF strength E over the allowable values E_{al} or even threshold breakdown values E_{br} in nearby volume of dielectric [2–6, 8].

In an alternating electric field pulsating pressures p and forces F arise from the direction of the water micro-inclusions towards the surface of the dielectric [2–6, 8]. At that the liquid inclusions cause the greatest pressures on its sharp poles that can exceed the mechanical strength of the polyethylene (elastic modulus of about 700 MPa) and lead to the appearance of micro-cracks. Conducting fluid filling micro-cracks increases the size and branching of the defects and as a consequence the region of the disturbed field also expands.

Changing the cross section of the conductor along the field, for example at the appearance of water micro-tree on the surface inclusion, leads to an increase in density of both the conduction current J_{cond} in local domain of inclusion and the displacement current J_{dis} in the nearby volumes of insulator [3–6]. This non-uniform current distribution throughout the volume of the material leads to an inhomogeneous dissipation of electrical energy in it, non-uniform heating of the dielectric and its local degradation.

Combined perturbations of electrical, mechanical and thermal fields in the solid dielectric can lead to both fast-deterministic degradation processes and slow stochastic ones in the strong EF [3–6]. For quantitative estimation of existent multi-physical processes it is necessary to determine the regularities of changes of maximal field strengths E_{max}, stressed volume V_{st}, electromechanical pressures p and the forces F, as well as the total current density J_{tot} in the dielectric depending on the configuration of its conducting micro-inclusions.

The aim of the work was to determine the regularities of local amplification of electrical, mechanical and thermal fields in the solid insulation, depending on the configuration of incipient conducting micro-inclusions, micro-juts and the micro-tree.

2. The physical and mathematical formulation of the problem

The formulation was performed by quasi-static approximation for non-ferromagnetic, linear and isotropic dielectric in a low-frequency harmonic electric field, as in [3−6]. The relationship of electromagnetic field parameters was described by system of Maxwell's equations [1, 2, 6] in the form of complex amplitudes for their deliverance from time dependence:

$$\mathrm{rot}\,\dot{\boldsymbol{H}} = \dot{\boldsymbol{J}}_{total}, \tag{1}$$

$$\mathrm{rot}\,\dot{\boldsymbol{E}} = -i\omega\,\dot{\boldsymbol{B}}, \tag{2}$$

$$\mathrm{div}\,\dot{\boldsymbol{B}} = 0, \tag{3}$$

$$\mathrm{div}\,\dot{\boldsymbol{D}} = \rho. \tag{4}$$

We neglected the time-lag effect, and the phase of field vectors at all medium points was taken the same. The external EF was accepted as vortex-free, therefore we introduced the scalar electric potential $\dot{\varphi}$, for which the equation is right (5):

$$\dot{\boldsymbol{E}} = -\mathrm{grad}\,\dot{\varphi}. \tag{5}$$

The computation equation for potential $\dot{\varphi}$ has the form [5, 7−10]:

$$\operatorname{div}\left[-\left(\gamma + i\omega\varepsilon_0\dot{\varepsilon}\right)\operatorname{grad}\,\dot{\varphi}\right] = 0 \qquad (6)$$

The so-called stressed dielectric volume V_{st}, i.e. the volume, in which the field strength E is larger than allowed value E_{al} for this insulator ($E > E_{al}$) for the three-dimensional computational model was determined according to the equation as in [5, 7−10]:

$$V_{st} = \int_V f(E)dV\ , \qquad (7)$$

where V is the calculated volume of the dielectric; $f(E)$ determines a function, which takes the value of $f(E) = 1$ for $E > E_{al}$ and $f(E) = 0$ for $E < E_{al}$.

The calculation of EF disturbances in dielectric with water micro-inclusions of different configuration was performed using the method of numerical finite elements. Conditions at the interface of the conductor-insulator (i.e. at the inclusion-medium interface) were determined for the potentials $\dot{\varphi}_1$ and $\dot{\varphi}_2$ as well as their derivatives in the direction of the normal to the interface surface [7−10]:

$$\dot{\varphi}_1 = \dot{\varphi}_2\,, \qquad (8)$$

$$\left(\gamma_1 + i\omega\varepsilon_0\dot{\varepsilon}_1\right)\partial\dot{\varphi}_1/\partial n = \left(\gamma_2 + i\omega\varepsilon_0\dot{\varepsilon}_2\right)\partial\dot{\varphi}_2/\partial n \qquad (9)$$

To obtain a unique solution of equation (6) on the upper and lower boundaries of the computational domain the Dirichlet conditions (potential values) were set, and on the lateral surfaces the Neumann conditions (the vanishing of potential derivative along the normal to the surface, i.e. the absence of currents in these directions) were involved.

For the calculation of force interactions of the micro-inclusions with the external EF and the insulation material the electric Maxwell stress tensor $\boldsymbol{T}$ was used, as in [8]. To find the electric force $\boldsymbol{F}$, acting on the volumetric element of inclusion dv from the field, it is necessary to calculate the cubic density of the force $\boldsymbol{f} = \rho\boldsymbol{E}$ and integrate it over volume dv. But in [3] it was proved, that the EF force effect on conducting inclusion can be regarded as the result of the forces, applied to the inclusion surface only. Therefore, the surface integral of the stress tensor $\boldsymbol{T}$ instead of the volumetric integral was used to determine the force $\boldsymbol{F}$ according to the expression:

$$\boldsymbol{F} = \iiint \boldsymbol{f}dv = \iint \boldsymbol{T}ds\ . \qquad (10)$$

The components of the volumetric force $\boldsymbol{f}$ in the coordinate axes can be written in terms of the field vector components [2]. For example, for the $\boldsymbol{f}_x$ component we could obtain the expression:

$$\boldsymbol{f}_x = \frac{\partial}{\partial x}\left[\frac{\varepsilon}{2}\left(\dot{\boldsymbol{E}}_x\overset{*}{\boldsymbol{E}}_x - \dot{\boldsymbol{E}}_y\overset{*}{\boldsymbol{E}}_y + \dot{\boldsymbol{E}}_z\overset{*}{\boldsymbol{E}}_z\right)\right] + \frac{\partial}{\partial y}\left(\varepsilon\dot{\boldsymbol{E}}_x\overset{*}{\boldsymbol{E}}_y\right) + \frac{\partial}{\partial z}\left(\varepsilon\dot{\boldsymbol{E}}_x\overset{*}{\boldsymbol{E}}_z\right) \qquad (11)$$

The equation for the tensor $\boldsymbol{T}$ components is given by:

$$\boldsymbol{T} = \begin{pmatrix} T_{xx} & T_{xy} & T_{xz} \\ T_{yz} & T_{yy} & T_{yz} \\ T_{zx} & T_{zy} & T_{zz} \end{pmatrix} = \qquad (12)$$

$$= \begin{pmatrix} \frac{\varepsilon}{2}\left(\dot{\boldsymbol{E}}_x\overset{*}{\boldsymbol{E}}_x - \dot{\boldsymbol{E}}_y\overset{*}{\boldsymbol{E}}_y - \dot{\boldsymbol{E}}_z\overset{*}{\boldsymbol{E}}_z\right) & \varepsilon\dot{\boldsymbol{E}}_x\overset{*}{\boldsymbol{E}}_y & \varepsilon\dot{\boldsymbol{E}}_x\overset{*}{\boldsymbol{E}}_z \\ \varepsilon\dot{\boldsymbol{E}}_y\overset{*}{\boldsymbol{E}}_x & \frac{\varepsilon}{2}\left(\dot{\boldsymbol{E}}_y\overset{*}{\boldsymbol{E}}_y - \dot{\boldsymbol{E}}_z\overset{*}{\boldsymbol{E}}_z - \dot{\boldsymbol{E}}_x\overset{*}{\boldsymbol{E}}_x\right) & \varepsilon\dot{\boldsymbol{E}}_y\overset{*}{\boldsymbol{E}}_z \\ \varepsilon\dot{\boldsymbol{E}}_z\overset{*}{\boldsymbol{E}}_x & \varepsilon\dot{\boldsymbol{E}}_z\overset{*}{\boldsymbol{E}}_y & \frac{\varepsilon}{2}\left(\dot{\boldsymbol{E}}_z\overset{*}{\boldsymbol{E}}_z - \dot{\boldsymbol{E}}_y\overset{*}{\boldsymbol{E}}_y - \dot{\boldsymbol{E}}_x\overset{*}{\boldsymbol{E}}_x\right) \end{pmatrix}$$

3. The results of the numerical experiment

The electric field distortions in the cross-linked polyethylene (XLPE) insulation of high-voltage cables with conducting water micro-inclusions of various configurations were simulated. The conducting fluid in such insulation can occur due to decomposition of the polymeric material components and as a result of the dielectrophoresis of water molecules along the conductor [10, 11]. The size, shape and mutual disposition of formed micro-inclusions are determined by the configuration of micro-pores and micro-cracks of the insulator, as well as the influence of electric forces of the external field.

3.1. Single micro-inclusions. We simulated the EF disturbances near the single water micro-inclusions with most characteristic shapes: a sphere, a rotation ellipsoid oriented along and across the field lines, an ellipsoidal micro-jut on a conductive surface and a sphere with unbranched water tree.

The simulation parameters were chosen as follows: sphere diameter d = 50 μm, ellipsoid semi-axes a_1 = 150 μm, $b_1 = c_1$ = 50 μm and $a_2 = b_2$ = 150 μm, c_2 = 50 μm, micro-jut height h = 75 μm, micro-tree length l = 75 μm, radius of its channel r_1 = 1 μm and the radius of the tip rounding r_2 = 1 μm.

Fig. 1 shows the EF inhomogeneous distribution in the XLPE insulation of high-voltage cable with mentioned conducting micro-defects.

Dark shading denotes the regions of the greatest EF amplification (over 50%), the field strength E value is determined according to the scale in Fig. 1 on the right. The length and direction of arrows correspond to the appearing electric force acting on the surface of the inclusions to the direction of the XLPE insulation material. The calculated values of maximum field strength E_{max} and the dielectric stressed volume V_{st} (when the field strength increases by 50 % and more) are shown in Table 1.

The maximum field strength E_{max} (in relative units, i.e. divided by the intensity E_0 of the undisturbed field) for the spherical micro-inclusions equals 3. For the ellipsoidal micro-inclusion and the micro-jut E_{max} ranges from 1 to 35, and for the sphere with tree it is equal to 50.

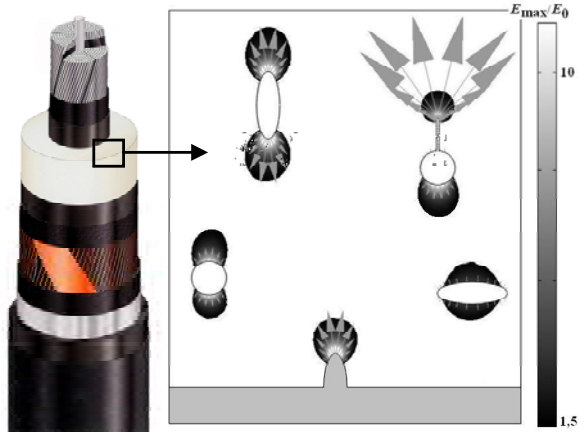

Fig. 1. EF inhomogeneous distribution in the XLPE insulation of high-voltage cable near different conducting micro-defects.

Table 1

The calculated values of E_{max} and V_{st}

	Sphere	Ellipsoid	Jut	Sphere with tree
E_{max}	3	1-35	1-35	to 50
V_{st},10^{-14} m^3	4,3	to 50,2	to 25,1	to 42,7

If the average field strength near the conductor of a high-voltage cable is about 10 kV/mm, E_{max} value grows to 350 – 500 kV/mm near the mentioned inclusions, which is 8−25 times higher, than polyethylene electric rigidity (20−40 kV/mm).

The dielectric stressed volume V_{st} for the sphere is equal to $4{,}3\cdot10^{-14}$ m^3, for the ellipsoid it is up to $50{,}2\cdot10^{-14}$ m^3, for the jut it comes up to $25{,}1\cdot10^{-14}$ m^3 and for a sphere with tree it reaches $42{,}7\cdot10^{-14}$ m^3. The expansion of V_{st} shows the increase in the dielectric breakdown probability in some point of stressed volume. If ρ is a probability density of the insulation breakdown, then the integral $P = \int \rho \, dV_{st}$ is equal to the probability of ubreakdown of this volume. If we take $P = 1$ at the critical value of stressed volume ($V_{st.cr}$ about 10^{-12} – 10^{-11} m^3 for XLPE insulation), the breakdown probability ranges from 4 to 50 % for the calculated V_{st}.

In the external EF the electric force ***F*** influences the charges induced on the conducting micro-inclusions surface. The surface density ***p*** of this force corresponds to the pressure of inclusions on the XLPE insulation material.

The calculated pressure p (see Fig. 1) depending on the micro-defect equals 0,01 to 10 MPa. The greatest $p \approx 10$ MPa is observed at the micro-tree tip and it is comparable with the mechanical strength of XLPE insulation (polyethylene breaking stress equals 9.8−16.7 MPa). In the alternating EF such power impacts occur with doubled frequency and, depending on the changes of inclusions configuration, can increase tenfold.

Calculated electric forces influence micro-inclusion poles and, depending on the micro-cavities configuration in dielectric, promote its stretching along the EF lines. Such deformation increases the EF disturbances, which is manifested by the increase of values E_{max}, V_{st}, F, and p. As it was mentioned above, the greatest values of E_{max} and p are observed at the water tree tip on the micro-inclusion surface. The character of EF amplification is defined by the proportion of dimensional parameters of such combined micro-inclusion. For the ellipsoid with unbranched cylindrical tree we identified five dimensional parameters: A and B denote the ellipsoid semi-axis across and along the EF lines, a is a tree radius and b is its half length, r is the radius of the tip rounding.

According to the results of [5, 7–10], it is known that the increase of the length of the inclusion and/or the tree along the field, as well as the tip rounding radius decreasing enhances the EF disturbances. Increasing both the inclusion dimensions (perpendicularly to the field) and tree thickness weakens the disturbances. For the quantitative estimation of the EF amplification we determined the influence of each of the dimensional parameters separately on the E_{max} value.

In Fig. 2, *a* dark shading shows the EF disturbance in dielectric near the tip of water tree. The graph in Fig. 2, *b* shows the E_{max} (normalized to E_0) dependence on each of the five dimensional parameters A, B, a, b and r of the combined inclusion.

The obtained dependencies with a high degree of accuracy can be approximated by the following exponential equations:

$$E_{max} = 14{,}02\, B^{\,0{,}45};$$
$$E_{max} = 13{,}91\, b^{\,0{,}42};\quad E_{max} = 12{,}78\, A^{\,-0{,}02};$$
$$E_{max} = 14{,}46\, r^{\,-0{,}27};\quad E_{max} = 11{,}09\, a^{\,-0{,}41}.$$

If the micro-inclusions the dimensions along the EF are larger than the micro-tree size, they are crucial to determine the character of the field disturbance. If the tree in the process of its elongation becomes larger than the inclusion, then tree dimensional parameters become the determining factor of the field disturbance.

The appearance of the micro-tree also has a significant influence on the distribution of conductivity current density J_{cond} along its channel and, consequently, on the magnitude of the displacement current in the dielectric J_{dis} at the tree tip. If for spherical inclusion the maximum current density $J_{max} = 5{,}5$ A/m^2, then for the ellipsoid J_{max} can amount to 80 A/m^2, and at water tree appearance J_{max} can increase up to values from 350 to 400 A/m^2.

Micro-tree configuration determines not only the value of J_{max}, but also the location of the areas of the greatest current density along the tree.

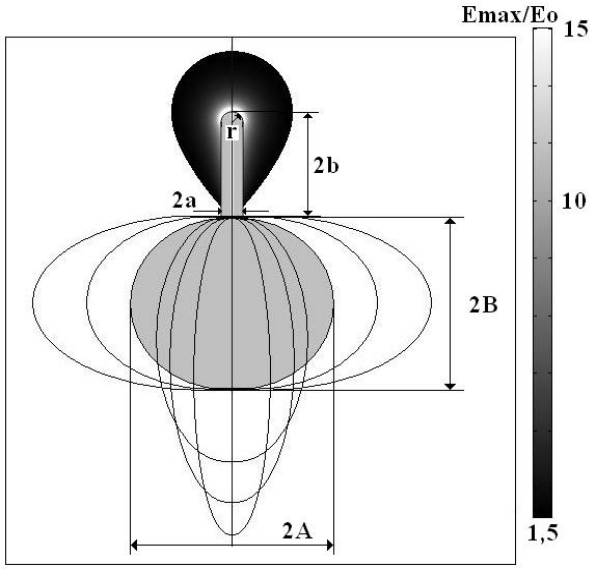

a

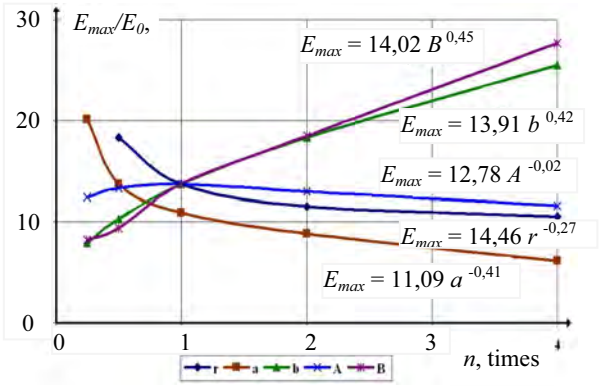

b

Fig. 2, a. EF disturbance near the tip of water tree.
b. Dependence of E_{max} on each of the five parameters.

Fig. 3, *a* and *b* shows the variation of the total current density J_{tot} along the water tree central channel with 50 μm length and in the volume of nearby dielectric depending on the micro-inclusion configuration.

In Fig. 3, *a* the curves 1, 2 and 3 correspond to the conical micro-tree with different angles α (from 1 to 5,5 deg.) of the channel incline to the tip.

Fig. 3, *b* shows the dependence of J_{tot} for the combined tree, 30 μm of which has a cylindrical form, and 20 μm has a conical one. As it can be seen from this figure, the current density at the tree bottom is independent of its configuration and equals 120 A/m^2. With the increase of the angle α of the tree conical part inclination, a current density at the tree tip grows from 150 to 350 A/m^2 (Fig. 3, *a*) and from 70 to 170 A/m^2 (Fig. 3, *b*).

Depending on the angle α, both the maximum current density J_{max} and the area of its observation are changed, i.e. J_{max} may be at the tree bottom, its middle or tip. Note that with the decrease in the rounding radius of the tree tip the value J_{max} can in addition increase up to 10 times.

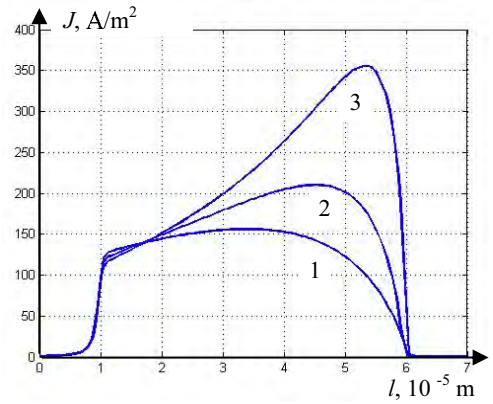

a

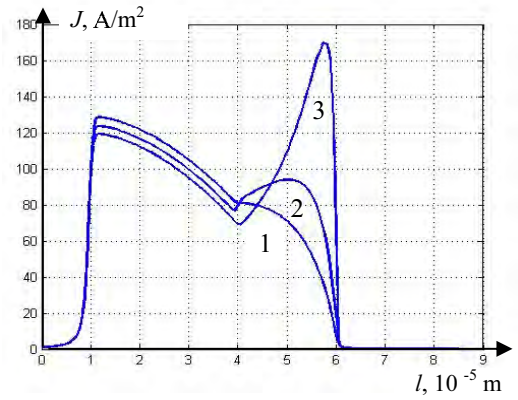

b

Fig. 3, a. Total current density J_{tot} along conical water tree.
b. J_{tot} along combined water tree.

Inhomogeneous distribution of J_{tot} in dielectric volume causes inhomogeneous heat energy dissipation in the dielectric and, as a consequence, heating up the inhomogeneous insulation. With the temperature increasing, the mechanical strength of XLPE insulation decreases. So when the temperature rises from 20 to 60 °C the polyethylene breaking stress decreases from 16,7–9,8 MPa to 3,3–8,8 MPa and the material ages intensively under the influence of pulsating forces exerted by the micro-inclusion.

3.2. Two closely located micro-inclusions. In the areas of the greatest EF amplification, that is, at the tips and the poles of micro-inclusions along the field, the concentration of moisture increases owing to dielectrophoresis of water molecules and the destruction of the polymer material. This can lead to the formation of micro-droplets of conductive fluid in the XLPE insulation of high-voltage cable, as shown in Fig. 4. Under the influence of electric forces of mutual attraction the drops unite and form closely located micro-inclusions (distance between the inclusions is less than their characteristic sizes).

As it is shown in [3–6], the amplification of the field in the XLPE insulation owing to such inclusions must be considered even if its maximum sizes are less than the ones allowable by known criteria.

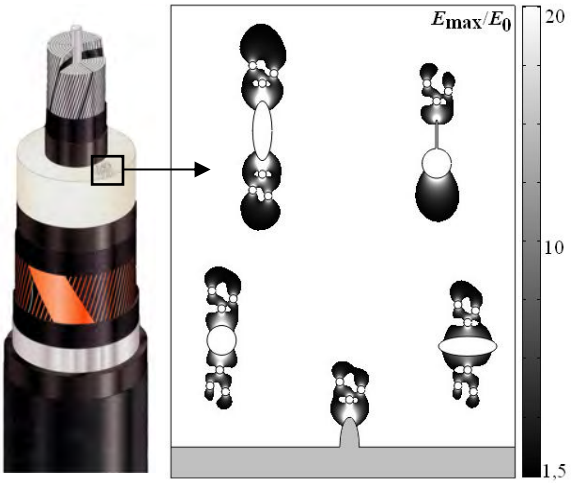

Fig. 4. Formation of micro-droplets of conductive fluid in the XLPE insulation of high-voltage cable.

We simulate a cumulative EF disturbance near two closely spaced micro-inclusions as well as the micro-inclusions and the micro-jut. The inclusions have the spherical shape with a diameter d = 50 μm or the ellipsoidal shape with the ratio a/c along and across the field from 1/10 to 10. Micro-jut height h = 75 μm, micro-tree length on the inclusions surface l = 75 μm, the radius of micro-tree channel r_1 = 1 μm and a radius of the rounding of the tip r_2 = 1 μm.

Fig. 5 shows the EF distortion in the dielectric near two closely located ellipsoidal micro-inclusions both without tree and with tree on the surface, as well as near the micro-jut and the ellipsoid. Shading areas correspond to areas of stressed volume V_{st}, the distribution of E corresponds to the scale in Fig. 5 on the right, and arrows depict the density vector of surface forces p.

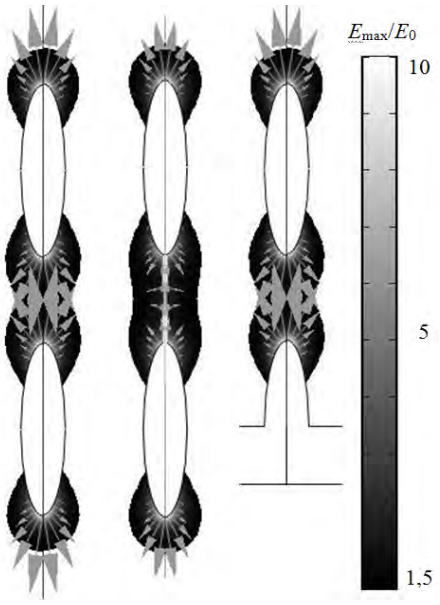

Fig. 5. EF distortion near two closely located ellipsoids.

According to the results of numerical experiments with decreasing distance l between the inclusions the EF in the dielectric gap may increase tenfold. So when l changes from 50 to 1 μm, E_{max} increases from 6 to 130 and J_{max} from 5 to 20 A/m^2. For example, if the average field strength at the core of a high-voltage cable with XLPE insulation is 10 kV/mm and in the space of 1 μm between the two elliptic inclusions it is amplified 130 times, i.e. E_{max} = 1300 kV/mm, this value is higher more than 30 times than the electric rigidity of polyethylene.

Electric charges induced at surface of closely located micro-inclusions interact not only with the external EF, but also with each other, being attracted to close poles. Density of charges on the opposite poles of the inclusions becomes non-symmetrical.

As the result, the distribution of the density of surface forces p also is non-symmetrical and there is resultant force F moving the inclusions in the strong field areas, i.e. initiating their mutual attraction.

Fig. 6 shows the dependence of the resulting force F of the mutual attraction of two spherical micro-inclusions on the distance between them.

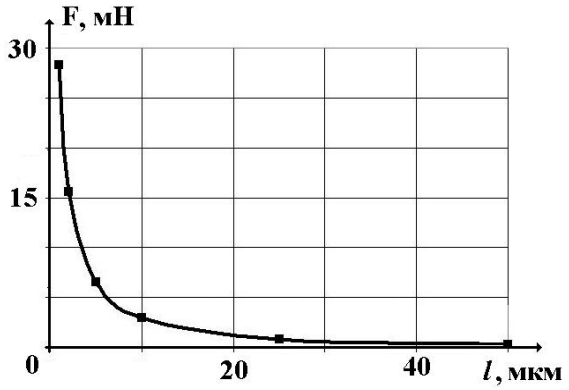

Fig. 6. F dependence on the distance between two inclusions.

With l decreasing, the value F increases according to the law of a power function and the approximation equation has the form $F = 36{,}46\ l^{-1.21}$. Due to the positive feedback during the long-term use of the XLPE insulation, its degradation will intensify the process of the approachment of micro-inclusions and EF amplification.

Over time, closely spaced water inclusions merge into total conductive channel along the field structure. As noted in [3–6], this configuration represents a significant danger for the XLPE insulation due to large EF distortions.

If the volume of appeared moisture in the XLPE insulation is not enough or configuration of the micropores of dielectric does not allow the formation of a new micro-inclusion, then liquid micro-droplets may contribute to the initiation of new branches of water tree.

The results of the numerical experiment on the calculation of the EF distortion near the micro-inclusion with trees of varying degrees of branching are shown in Fig. 7.

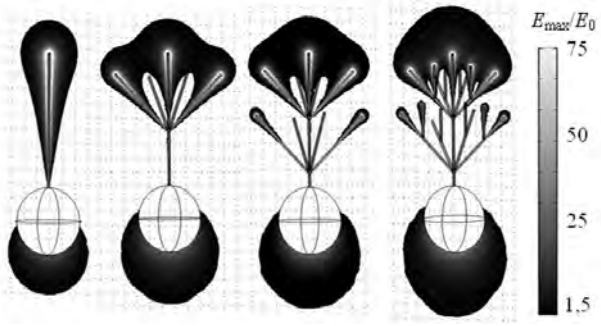

Fig. 7. EF distortion near the tree of varying branching.

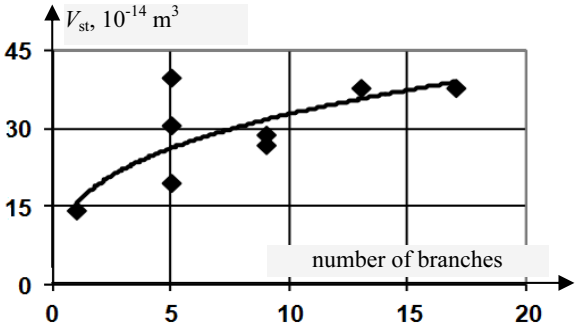

Fig . 8. V_{st} as a function of number of branches of tree.

The micro-inclusion has a spherical shape with a diameter d = 50 μm, micro-tree length l = 100 μm, the radius of each of the cylindrical branches r_1 = 1 μm and the radius of tip rounding r_2 = 1 μm. Shading areas correspond to areas of stressed volume V_{st}, and the distribution of field strength E is determined according to the scale on the right.

According to the calculations, branching of the tree reduces E_{max} on its tip owing to screening of the induced charges on the central branch by other closely spaced branches. This result agrees well with [5, 6, 8], where it is reported that intensive branching of tree leads to delay and even to a complete stop of its growth.

But, despite the decrease in E_{max}, value of V_{st} increases. Fig.8 represents a plot of the value of V_{st} as a function of the number of tree branches.

The more tree branches the more areas with increased strength are in the nearby XLPE insulation and, as a result, the greater breakdown probability. If the breakdown probability of the dielectric local volume at the tree branch tip is 5 %, then in the presence of 17 branches (case 4 in Fig. 7) the breakdown probability of any of these local volumes becomes $1 - 0{,}95^{17} = 0{,}58$, i.e. 58 per cent.

Besides, when tree branches, the number of areas with increased pressures p (see Fig. 9) and higher total current density J_{tot} are respectively increased this, in addition to the electrical aging, results in mechanical and thermal degradation of dielectric.

Also the EF distortion produced by two closely spaced spherical micro-inclusions with branched micro-trees on its surfaces has been simulated. Fig. 10 shows the resulting V_{st} areas and the pressure p vectors of the liquid on the dielectric surface.

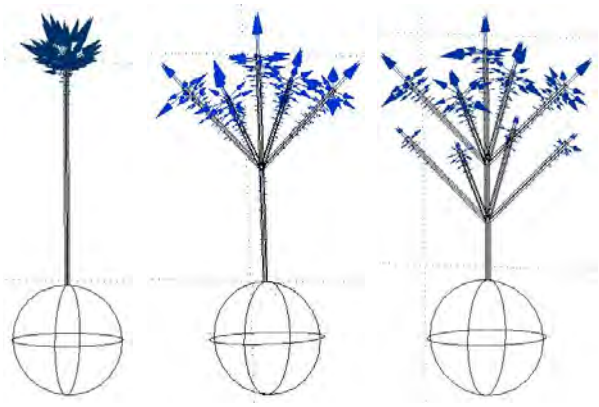

Fig. 9. Areas of increased pressures p near the branched tree.

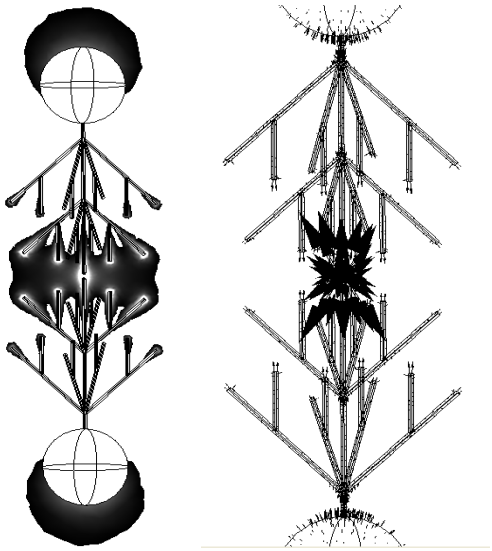

Fig. 10. Vst areas and the pressure p near two closely spaced inclusions with branched micro-trees on its surfaces.

In this case the greatest field amplification arises between tree tips, i.e. in the center of the dielectric gap, unlike two inclusions without trees, where the maximum field amplification arises at the surfaces of their poles.

Thus, the presence of closely spaced micro-inclusions and branched micro-trees on dielectric surfaces can amplify E_{max} up to 130 times as well as increase both V_{st} and the number of dangerous areas with heightened strength, pressures and current densities in insulation. This intensifies its degradation processes and the breakdown probability.

3.3. Groups of closely spaced micro-inclusions. Under the influence of electrical forces the conductive fluid volume in the solid dielectric spreads in the form of fine droplets (of micron sizes) over a larger volume instead of forming a few large particles. Although the size of each separate inclusion is much less than the acceptable size according to quality criteria of XLPE

insulation, the accumulation of the group (cloud) of closely spaced inclusions is dangerous [3–6].

We also investigated the dependence of EF amplification degree on the dispersion of the inclusions, i.e. the quantity of inclusions at the constant total volume of conductive liquid.

In Fig. 11, *a* dark shading shows the V_{st} areas near to one, three and five spherical micro-inclusions and five ellipsoidal ones. The sphere diameters and the ellipsoid semi-axes were chosen so that the total volume of liquid remained invariable.

The graph Fig.11, *b* depicts the dependence of the V_{st} in dielectric on the number of micro-inclusions at distances l_1 = 50 μm and l_2 = 100 μm between them. The regularity of the stressed volume growth with the increasing of dispersiveness of inclusions system was shown.

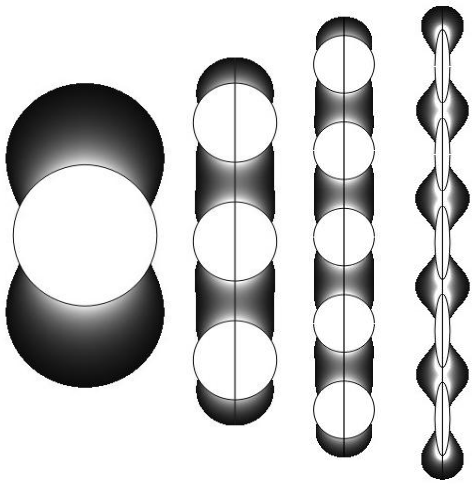

A)

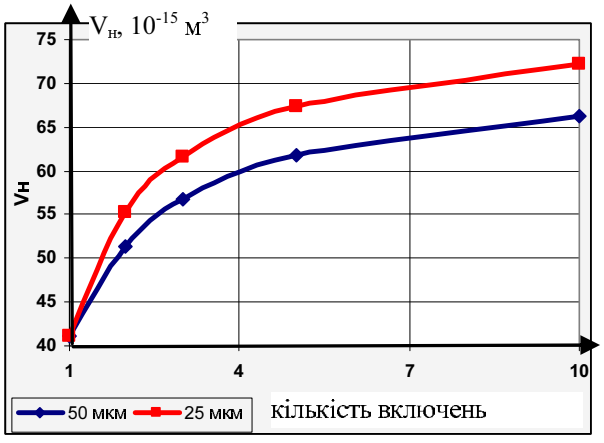

b)

Fig. 11. V_{st} areas near to one, three and five inclusions(a);. V_{st} dependence on the number of inclusions (b).

Thus configuration of micro-inclusions in comparison with two closely spaced ones is characterized by a large number of areas with heightened strength E_{max}, pressure p_{max} and current J_{max}. If for two inclusions only one dielectric gap with possible degradation processes in insulation exists, then for five micro-inclusions four such gaps were determined.

4. Conclusion

The combined mechanism of electric field distortion and amplification of electrical strength, mechanical and thermal intensities in the solid dielectric, depending on the configuration of its conducting micro-inclusions is studied.

The greatest amplification of the maximum field strength (8 to 25 times higher than electric strength of polyethylene), electrical forces and pressures (up to 10 MPa) is caused by strongly extended along the field ellipsoidal micro-inclusions and micro-juts as well as by micro-inclusions with the water tree on the surface.

The appearance of the tree on the surface of the micro-inclusion can increase the total current density in the dielectric (up to 100 times), that contributes to its inhomogeneous heating and mechanical strength reduction (in 2–3 times). It also can create pulsing forces comparable to the strength limit of the crosslinked polyethylene.

The appearance of the group of closely spaced micro-inclusions as well as water tree branching increases the number of areas with disturbed electrical, mechanical and thermal fields in the dielectric, and therefore, increases the total probability of threshold-breakdown processes of XLPE insulation at least in one of these areas.

The analysis of deterministic and stochastic processes of solid dielectric aging in a strong electric field shows the combined mechanism of dielectric degradation, positive processes feedback and the necessity of finding solutions to interrelated problems for the accurate evaluation of disturbance character.

References

[1] L. A. Dissado, “Understanding Electrical Trees in Solids: From Experiment to Theory”, *IEEE Trans. on DEI*, vol. 9, pp. 483–497, 2002.

[2] L. D. Landau and E.M. Lifshyts, *Electrodynamics of continuums*. Moscow, Russia: Nauka, 1980. (Russian)

[3] J. J. O'Dwyer, “The Theory of Electrical Conduction and Breakdown in Solid Dielectrics” Oxford, UK: Clarendon Press, 1973.

[4] E. O. Forster, “Progress in the Understanding of Electrical Breakdown in Condensed Matter”, *J. Phys., D: Appl. Phys.* vol. 23, pp. 1506–1514, 1990.

[5] A. A. Shcherba, A. D. Podoltsev, and I. N. Kucheriava, “Electromagnetic processes in the polyethylene insulated cable line for voltage 330 kV”, *Tekhnichna Elektrodynamika,* vol. 1, pp. 9–15, 2013. (Russian)

[6] N. Shimizu and H. Tanaka, "Effect of Liquid Impregnation on Electrical Tree Initiation in XLPE", *IEEE Trans. DEI*, vol. 8, pp. 239–243, 2001.

[7] M. A. Shcherba, *Electric field distortion by conducting inclusions in dielectrics*. Kyiv, Ukraine: Institute of Electrodynamics of National Academy of Sciences of Ukraine, p. 223, 2013.

[8] M. A. Shcherba, "The force interaction between close placed conducting micro-inclusions in dielectric medium under the external electric field", *Tekhnichna Elektrodynamika*, vol. 3, pp. 11–13, 2012. (Russian)

[9] M. A. Shcherba, "Dependences of electric field amplification during water tree branching in solid dielectrics", in *Proceedings of the IEEE International Conference on Intelligent Energy and Power Systems (IEPS)*, pp. 46 – 49, Kyiv, Ukraine, 2014.

[10] A. K Shydlovskii ., A. A.Shcherba, V. M. Zolotarev, A. D. Podoltsev, I.N.Kucheriava, *Cables with polymer insulation on extra high-voltage*. Kyiv, Ukraine: Nash format, p. 550, 2013. (Russian)

[11] H. R. Zeller, "Breakdown and prebreakdown phenomena in solid dielectrics", *IEEE Trans. Elect. Insul.*, vol. EI-22, no. 2, pp. 115–122, 1987.

ВЗАЄМОПОВ'ЯЗАНІ ПРОЦЕСИ ЛОКАЛЬНОГО ПІДСИЛЕННЯ ЕЛЕКТРИЧНОГО ПОЛЯ В ТВЕРДИХ ДІЕЛЕКТРИКАХ, ЯКІ ПРИСКОРЮЮТЬ ЇХ ДЕГРАДАЦІЮ

Максим Щерба

Описано особливості локального підсилення електричного поля, а також електричних, механічних і термічних напруженостей у твердому діелектрику в залежності від конфігурації його провідних мікровключень. Проведено аналіз умов збільшення максимальної напруженості поля, напруженого об'єму, електромеханічних тисків, сил і густини повного струму в діелектрику як основних факторів, що визначають детерміновані та стохастичні процеси його деградації в збуреному гармонічному електричному полі.

Maksym Shcherba – graduated from "Kyiv Polytechnic Institute" National Technical University, Ukraine (M. Sc. in Applied Physics). He defended Ph. D. thesis in Theoretical Electrical Engineering at the Institute of Electrodynamics of the National Academy of Sciences of Ukraine. He works at the Department of Theoretical Electrical Engineering of "Kyiv Polytechnic Institute" NTUU as a Senior Lecturer. IEEE member.